
EMOTION RECOGNITION IN TALKING-FACE VIDEOS USING PERSISTENT ENTROPY AND NEURAL NETWORKS

A PREPRINT

Eduardo Paluzo-Hidalgo
Applied Math I department
University of Sevilla
epaluzo@us.es*

Guillermo Aguirre-Carrazana
University of Sevilla
kaprekar.aguirre@gmail.com

Rocio Gonzalez-Diaz
Applied Math I department
University of Sevilla
rogodi@us.es

October 27, 2021

ABSTRACT

The automatic recognition of a person's emotional state has become a very active research field that involves scientists specialized in different areas such as artificial intelligence, computer vision or psychology, among others. Our main objective in this work is to develop a novel approach, using persistent entropy and neural networks as main tools, to recognise and classify emotions from talking-face videos. Specifically, we combine audio-signal and image-sequence information to compute a *topology signature* (a 9-dimensional vector) for each video. We prove that small changes in the video produce small changes in the signature. These topological signatures are used to feed a neural network to distinguish between the following emotions: neutral, calm, happy, sad, angry, fearful, disgust, and surprised. The results reached are promising and competitive, beating the performance reached in other state-of-the-art works found in the literature.

1 Introduction

Facial emotion recognition consists of a series of processes to detect human emotions from facial human expressions. When people communicate with others, they are constantly sending and receiving nonverbal cues, expressed through body gestures, voice, facial expressions, and physiological changes. Nonverbal cues increase the trust, clarity and provide more information supporting what spoken words transmit. A particular emotional state produces certain verbal and nonverbal signals that transmit the information regarding personal feelings.

Nowadays, (facial) emotion recognition has become an important research area in the fields of computer vision and artificial intelligence due to its potential applications. In general, people express their emotional state (such as joy, sadness, or anger) through facial expressions and vocal tones and these are the features that are often analyzed for emotion recognition. So far, different approaches have been explored. For example, in the H2020 KRISTINA project², computer-aided emotion recognition is used to help in the interaction between health professionals and migrated patients, allowing to overcome linguistic barriers that hinder communication. In addition to the KRISTINA project, other European projects working on emotion recognition are, for example, the VocEmoApI project³ and the MixedEmotions project⁴. The VoicEmApI project developed a software for the detection of vocal emotion focused on extracting vo-

*Corresponding author.

²<http://kristina-project.eu/en/>

³https://cordis.europa.eu/project/rcn/199804_es.html

⁴https://cordis.europa.eu/project/rcn/194226_es.html

cal markers that are caused by changes in physiological processes such as the cognitive affective process. Acoustic voice analysis works with the basic components of emotional processes, for example, a person’s evaluation of relevant events or situations that could trigger actions and expressions that constitute an emotional episode. These evidences were continuously tracked. The project deduced not only basic emotions, but also much finer distinctions, such as sub-categories of emotions and subtle emotions. The project conducted its impact to large markets such as home robotics, public safety, clinical diagnosis and therapy, call analysis and market research. On the other hand, the MixedEmotions project developed an application based on a more complete emotional profile of the person’s behavior. It used data from different channels: multilingual text data sources, audio and video signals, social media and structured data. The project offered commercial solutions providing an integrated big linked data platform for emotional analysis using heterogeneous sets of data and addressing the multilingual and multimodality aspects in a robust and large-scale setting.

Regarding computer-aided emotion recognition research works, roughly speaking, they are focused on the use of various input types such as facial expressions Ofodile et al. [2017], Shojaeilangari et al. [2016], Wan et al. [2017], speech Plawiak et al. [2016], Sapiński et al. [2018], Kleinsmith and Bianchi-Berthouze [2012], Noroozi et al. [2018], Avots et al. [2019] and physical signals Jenke et al. [2014].

Furthermore, several classification and recognition techniques have been proposed in the past. Some of them used speech prosody contours information to recognize emotions through different classification methods such as artificial neural networks, multi-channel hidden Markov models, mixture of hidden Markov models, and, Active Appearance Models (AAMS). Lately, hybrid neural networks combining convolutional neural networks and recurrent neural networks have become the state-of-art for emotion recognition. For example, the authors in Guo et al. [2020] proposed an audiovisual-based hybrid network that combines the predictions of five models for emotion recognition in the wild. The overall accuracy of the proposed method achieved 55, 61% and 51, 15% classification accuracy for the audio-only and video-only dataset, respectively. The authors used the Afew-va Database for Valence and Arousal Estimation In-the-wild introduced in Kossaifi et al. [2017]. The authors in Issa et al. [2020] faced the task of audio emotion recognition using a convolutional neural network. Their baseline model included one-dimensional convolutional layers combined with dropout, batch normalization, and activation layer. The proposed framework achieved 71.61% of accuracy for the Ryerson Audio-Visual Database of Emotional Speech and Song (RAVDESS dataset) (see Livingstone and Russo [2018]). Later, in Kwon et al. [2021], a new preprocessing scheme is proposed in order to remove the noise from speech signals based on fast Fourier transformation and spectral analysis. The authors evaluated their model using benchmark IEMOCAP and EMODB datasets and obtained a high recognition accuracy, which were 73% and 90%, respectively. Finally, in Gonzalez-Diaz et al. [2019], a persistent-topology-based method is developed to obtain a single value for the audio signal of a given video of a person expressing emotions. These data were later used as the input of a support vector machine to classify audio signals into eight different emotions, namely, neutral, calm, happy, sad, angry, fearful, disgust, and surprised. The results obtained were close to the existing accuracy of methods with a greater scope such as the ones introduced in Kryzhanovskiy et al. [2017], Zhang et al. [2015].

This paper can be considered a continuation of the work developed in Gonzalez-Diaz et al. [2019]. Here, instead of dealing with the audio signals only, we deal with talking-face videos. The method incorporates the idea from Gonzalez-Diaz et al. [2019] for audio-signal emotion classification that consists of computing the persistent entropy (introduced in Chintakunta et al. [2015]) of the lower-star filtration of the 1-dimensional simplicial complex obtained by a discretization of the audio signal, together with the idea from Lamar-Leon et al. [2016] for gait classification that consists of computing a 3-dimensional simplicial complex from the given image sequence, and extracting eight different topological features from eight different filtrations considering, respectively, the distance to eight fixed planes (two horizontal, two vertical and four obliques). This way, the method is able to completely capture the movement in the image sequence. This methodology were also used in Lamar-León et al. [2014] to monitor human activities at distance and in Lamar-León et al. [2013] for gait-based gender classification. Persistent entropy has been widely used in very different situations. For example, in Chung et al. [2021], it is used to measure the heart rate variability to a sleep-wake classification. In Myers et al. [2019], it is used to detect dynamic states, and, in Ruocco et al. [2020], to detect glioblastomas. Specifically, the persistence barcode (or diagram) (a key tool in computational topology Edelsbrunner and Harer [2010]) is used to compute the persistence entropy and, for the application considered in this paper, persistence barcodes have a clear interpretation as the gestures will modify the birth and death of the different connected components obtained from the facial landmark points through the considered filtration. The novelty of the method presented here is the combination of the previous ideas with a particular construction of the 3-dimensional cell complex and the use of the result to feed a neural network. Specifically, given a talking-face video, instead of segmenting each image of the image sequence as it is done in Lamar-Leon et al. [2016], we use precomputed landmark points to build the 2-dimensional Delaunay triangulation in each frame of the given image sequence and then stack them in a particular way to build a 3-dimensional cell complex. Later, we compute the persistent entropy of each of the eight filtrations. The computed topological features together with the feature obtained from the audio-signal

following Gonzalez-Diaz et al. [2019], make up a 9-dimensional vector also called topological signature. Besides, thanks to Atienza et al. [2020], we are able to prove that the topological signatures are stable to small changes in the input audio signal and image sequence. Finally, the topological signatures computed are used to train a neural network to classify emotions. Let us observe that the neural network considered in this paper is extremely simple because of the low dimension of the input. This methodology has been tested using the RAVDESS dataset Livingstone and Russo [2018] showing that our results outperform state-of-the-art methods.

The paper is structured as follows. The needed background is introduced in Section 2. The description of the proposed method is provided in Section 3. The experimentation made is presented in Section 4, together with comparisons with state-of-the-art methods. Finally, Section 5 provides conclusions and future work ideas.

2 Background

In this section, the main concepts from topological data analysis and neural networks, needed to understand our method for facial emotion recognition, are recalled.

2.1 Topological data analysis

Topological data analysis has emerged as an important approach to characterize the behavior of datasets using techniques from topology. Tools from topological data analysis, specifically persistent homology, allow assigning shape descriptors to large and noisy data across a range of spatial scales. Assuming that the input data are sampled from an underlying space \mathbb{X} and that the aim is to recover the topology of \mathbb{X} , a general topological data analysis process follows these steps:

1. Find an approximation of \mathbb{X} using a combinatorial structure.
2. Compute topological features of such structure such as persistent homology.
3. Summarize the topological features computed using statistical tools such as persistent entropy.

The combinatorial structure used in this work to represent objects is the one of cell complexes, whose elements in each dimension d , called d -cells, are d -dimensional topological spaces homeomorphic⁵ to a d -dimensional ball. This way, a 0-dimensional cell is a point (vertex), a 1-dimensional cell is a curve, a 2-dimensional cell is homeomorphic to a disk and so on. A *cell complex* K is a collection of cells constructed inductively: (1) The 0-skeleton $K^{(0)}$ (i.e., the set of 0-cells of K) are a set of points in an ambient n -dimensional space \mathbb{R}^n . (2) Form the d -skeleton $K^{(d)}$ from the $(d-1)$ -skeleton $K^{(d-1)}$ by attaching d -cells via homeomorphisms.

From now on, we will assume that the given cell complex K has a finite number of cells. The boundary set of a d -cell $\sigma \in K$ can be informally defined as the set of $(d-1)$ -cells in the $(d-1)$ -skeleton $K^{(d-1)}$ used to attach the d -cell σ . Successively adding to $F = \{\sigma\}$ the boundary set of each cell in F , we obtain the faces of σ . For example, the boundary set of an edge is its two endpoints (vertices). A maximal cell of K is a cell not in the boundary of any other cell of K . A d -dimensional cell complex K is a cell complex satisfying that the dimension of the cell of the higher dimension in K is d . A subcomplex of a cell complex K is a subset $K' \subset K$ which itself is still a cell complex. An example of a subcomplex is the closed star of a vertex v , denoted by $\text{St } v$ and defined as follows: A cell σ is in $\text{St } v$ if there exists $\mu \in K$ such that σ and v are faces of μ . A filtration is an increasing sequence of cell complexes $\emptyset \subseteq K_1 \subset K_2 \subset \dots \subset K_r = K$. A particular case of cell complexes is the one of simplicial complexes. For any dimension d , a d -simplex is the convex hull of $d+1$ affinely independent points v_0, v_1, \dots, v_d living in the n -dimensional space \mathbb{R}^n with $d \leq n$. See an example of a filtration of simplicial complexes in Figure 1.

There are several methods to compute cell complexes and filtrations from input data depending on the nature of the data and the purpose of the analysis. In this work, we will use the following process to produce simplicial complexes from data: Consider a set of points S in \mathbb{R}^n . Define V_s as the set of points of \mathbb{R}^n that are closer to $s \in S$ than to any other point of S . That is, for $s \in S$, $V_s = \{x \in \mathbb{R}^n \mid d(x, s) \leq d(x, s') \forall s' \in S\}$. The collection of the sets V_s is a covering for \mathbb{R}^n and it is called the Voronoi decomposition of \mathbb{R}^n concerning S . The nerve of this covering is a simplicial complex called the Delaunay triangulation of S . The construction of this complex is costly in high dimensions, although there exist efficient algorithms for computing it when $n = 2$ and $n = 3$. See Toth et al. [2017] for more details on Voronoi diagrams and Delaunay triangulations. The filtration considered in this paper is the lower-star filtration. Let us see how to define it. Consider a real-valued function h on a finite set of points $V \subset \mathbb{R}^n$. Suppose K is a cell complex with set of vertices V . The lower star of $v \in V$ is defined as the subset of cells of K for which v

⁵A homeomorphism is a bicontinuous and bijective function between two topological spaces.

is the vertex with maximum function value, that is, $\text{low St } v = \{\sigma \in \text{St } v : x \in \sigma \Rightarrow h(x) \leq h(v)\}$. Sort the vertices by their function values, in a non-decreasing order, $V = \{v_1, v_2, \dots, v_r\}$. The lower-star filtration (see [Edelsbrunner and Harer, 2010, page 135]) $\emptyset \subseteq K_1 \subset K_2 \subset \dots \subset K_r = K$ satisfies that K_j is the union of the lower stars of the first j vertices of V , that is, $K_j = \bigcup_{i \leq j} \text{low St } v_i$, for all j . Once we have computed a filtration, the next step is to compute topological features from it, such as the homology. The d -dimensional homology group of a topological space represents its d -dimensional holes. Intuitively, a 0-dimensional hole is a connected component, a 1-dimensional hole is a tunnel and a 2-dimensional hole is a cavity. Classical results ensure that d -dimensional homology groups are topological invariant, that is, they are invariant under homeomorphisms. The d -dimensional homology group of a topological space structured as a cell complex K can be defined as follows. First, the d -dimensional chain group $C_d(K)$ is obtained by summing up d -cells⁶. Then, the boundary operator is extended to a linear map ∂_d from $C_d(K)$ to $C_{d-1}(K)$ in the obvious way. Since the boundary of the boundary of a cell is always zero, then the image $B_d(K)$ of ∂_{d+1} is a subgroup of the kernel $Z_d(K)$ of ∂_d and then, the d -dimensional homology group of K is the quotient group $H_d(K) = B_d(K)/Z_d(K)$. An element α of $H_d(K)$ is called a d -dimensional homology class of K .

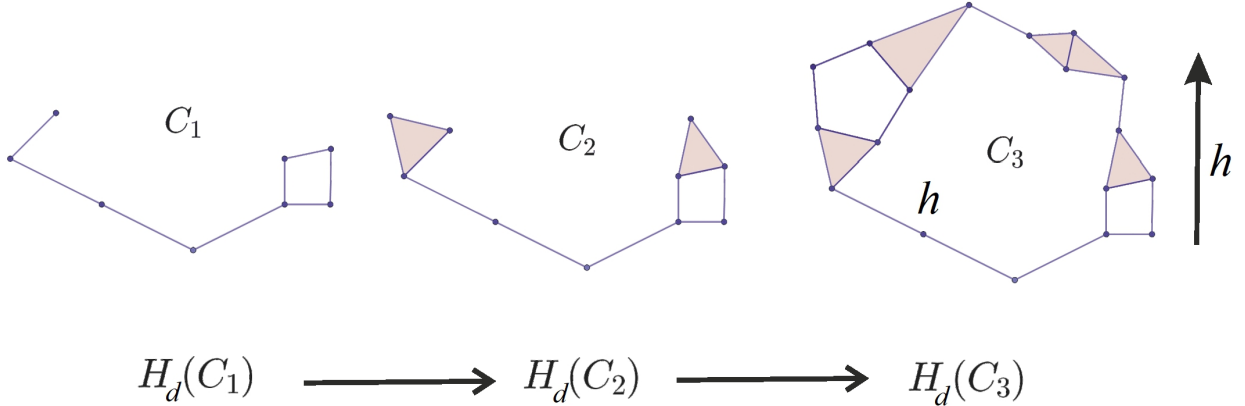


Figure 1: Top: Example of a filtration obtained using the height function h on its vertices. Bottom: Associated d -dimensional persistent homology. For example, if $d = 1$ then $H_1(C_1) = \mathbb{Z}_2 \xrightarrow{[1]} H_1(C_2) = \mathbb{Z}_2 \xrightarrow{[1 \ 0]} H_1(C_3) = \mathbb{Z}_2 \oplus \mathbb{Z}_2$

Although the concept of homology is not useful in practice due to its lack of discrimination, this notion is used in Edelsbrunner and Harer [2010] to define a more discriminant concept called persistent homology, together with an efficient algorithm to compute it. Later, in Zomorodian and Carlsson [2005], the initial definition is reformulated. The persistent homology of a filtration tracks the moment i where a homology class is born and the moment j where the same class dies leading to a topological descriptor called persistence diagram. For example the lower-star filtration leads a family $\{H_d(K_t) : t \in \mathbb{R}\}$ of homology groups and the inclusions $K_t \hookrightarrow K_s$ lead a family of homomorphisms $\{H_d(K_t) \rightarrow H_d(K_s) : t \leq s\}$, for $d \in \mathbb{Z}$. Now, each homology class α that was born in $H_d(K_t)$ and died in $H_d(K_s)$ can be stored as a point (t, s) . The result is a multi-set of points in \mathbb{R}^2 called the persistence diagram for the given filtration. The persistence of the homology class α is the difference $\text{pers}(\alpha) = s - t$. Then, homology classes with infinity persistence correspond to points of the form $(t, +\infty)$. In this work, points of the form $(t, +\infty)$ are replaced by points of the form $(t, N + 1)$, where N is a fixed big positive integer. This way, all points in the persistence diagram have finite coordinates. The features of higher persistence are represented by the points furthest from the diagonal while nearby points to the diagonal may be interpreted as topological noise.

In Turner et al. [2014], Munch et al. [2015], Chazal et al. [2013] among others, persistence diagrams are studied from a probabilistic and statistical point of view. In this paper, we summarize the information described by a persistence diagram in a number called persistent entropy (introduced in Chintakunta et al. [2015]) which consists in the Shannon entropy of the probability distribution obtained from the given persistence diagram. There are many applications of persistent entropy. For example, in pattern recognition Merelli et al. [2016], Rucco et al. [2017], complex systems Binchi et al. [2014], Myers et al. [2019], time series Chung et al. [2021], and clustering Wang et al. [2017]. Given a filtration and the corresponding persistence diagram $\text{Dgm} = \{(a_j, b_j) : j \in J\}$, the persistent entropy of the filtration is defined as $E = -\sum_{j \in J} p_j \log(p_j)$ where $p_j = \frac{\ell_j}{L}$, $\ell_j = b_j - a_j$, and $L = \sum_{j \in J} \ell_j$. Let us notice that if

⁶The ground ring considered in this paper is \mathbb{Z}/\mathbb{Z}_2 .

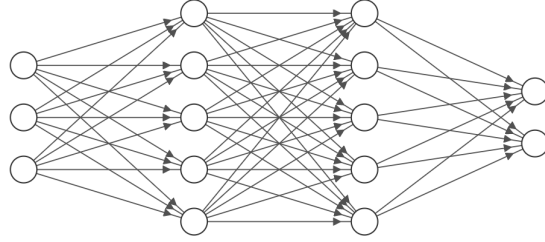


Figure 2: A $3 \times 5 \times 5 \times 2$ feedforward neural network composed of an input layer with 3 neurons, two hidden layers with 5 neurons each, and an output layer with 2 neurons.

$p_j \leq 1$, then $\log(p_j) \leq 0$, so the persistent entropy is always positive. Intuitively, the persistent entropy measures how different the persistence of the homology classes that appear along the filtration are.

2.2 Neural Networks

In this paper, we deal with a supervised classification problem where a set of labelled examples are provided with the aim of making predictions for unlabelled points. A widely extended machine learning model for classification problems is neural networks. In general, we could say that a neural network is a mapping $\mathcal{N}_{\omega, \Phi} : \mathbb{R}^n \rightarrow \mathbb{R}^m$ that depends on a set of weights ω and a set of parameters Φ describing the synapses between neurons, layers, activation functions and any other characteristic of its architecture. A good introduction to artificial neural networks was given in Haykin [2009]. A specific kind of neural network architecture is a feedforward neural network composed of a set of neurons hierarchically organized in layers that are fully connected as the example displayed in Figure 2. Neural networks can be seen as directed graphs where the input is transmitted and transformed along the graph using different operations. In each neuron (represented as a node of the graph), an activation function such as ReLu, sigmoid or softmax is applied.

To train the neural network $\mathcal{N}_{\omega, \Phi}$ for a supervised classification task, we will use a labelled dataset $D = \{(x, c_x)\}$ consisting of a finite set of pairs where, for each pair (x, c_x) , point x lies in \mathbb{R}^n and label c_x lies in $\{0, 1, \dots, k\}$, for some $k \in \mathbb{N}$. During the training process, the set of weights of the neural network is updated trying to minimize a loss function which measures the difference between the output of the network (obtained with the current weights) and the desired output (dictated by the labelled dataset). The loss function used in this paper is the cross-entropy loss function which is related to the Kullback-Leibler divergence: Given two probability distributions $P(x)$ and $Q(x)$ over the same random variable x , the cross-entropy is computed as $H(P, Q) = -\sum_{(x, c_x) \in D} P(x) \log(Q(x))$. To iteratively update the weights, the loss-driven training method used in this paper is the Adam algorithm (introduced in Kingma and Ba [2017]) which is a stochastic gradient-based optimization algorithm.

The goal of training a neural network is generalization. That is, we want our neural network to learn from the given data and to apply the learnt information on new data. One way to measure the performance of the trained neural network is to split the given dataset into two subsets called the training set and the test set. When the trained neural network reaches high accuracy on the training set but performs badly on new data, we say that there is an overfitting. There are different approaches to prevent overfitting such as dropout that consists in invalidating randomly a certain percentage of the neurons of the neural network during the training procedure (consult Srivastava et al. [2014] for more information).

3 Description of the method

In this section, we develop an emotion recognition method using persistent entropy and neural networks as main tools. Overall, the method works as follows. The input data are talking-face videos with precomputed facial landmark points. For each video, we compute a topological feature obtained from the audio signal together with eight topological features obtained from the image sequence, deriving a 9-dimensional vector call the topological signature of the video. The set of topological signatures obtained from the video dataset will then be used to feed a neural network.

We start the procedure by extracting the landmark points on each frame of the input image sequence (see Figure 3). we assume that these landmark points are already precomputed in the given dataset.

Given an image sequence obtained from a talking-face video with landmark points precomputed, we compute, for each frame, the 2-dimensional simplicial complex consisting of the Delaunay triangulation of the set of points cor-

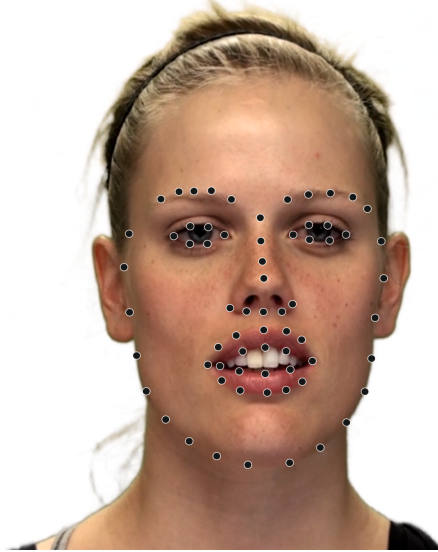


Figure 3: The landmark points considered in this paper, drawn on a face in one frame of a video from the RAVDESS dataset.

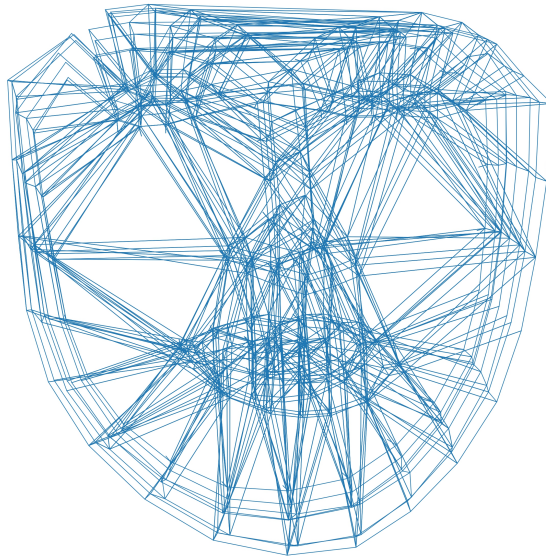


Figure 4: The 1-skeleton of the cell complex obtained from an image sequence.

responding to the spatial position of the landmark points. In order to connect the topological information along the image sequence, the landmark points corresponding to the same part of the face in consecutive frames are joined by an edge. A 2-dimensional cell is obtained when the two endpoints of an edge are joined to the two endpoints of the corresponding edge in the neighbor frame. A 3-dimensional cell is obtained when the vertices of a triangle of the Delaunay triangulation associated to one frame are joined with the vertices of the corresponding triangle in the neighbor frame. The output of the steps described in this section is a 3-dimensional cell complex K for each input image sequence which condenses all the gestures the person is making while recording on video. See Figure 4, where the 1-skeleton of the 3-dimensional cell complex K obtained from an image sequence is pictured.

The next step in this process is to sort the cells of K in order to obtain a filtration. In this work, eight different filtrations (two horizontal, two vertical, and four obliques) are used to obtain eight different persistence diagrams (see Figure 5 to have intuitions). The filtrations will capture the small movements of the landmark points through the given image sequence. The way to define a filtration is as follows: Given a plane π , we define the filter function $h_\pi : K \rightarrow \mathbb{R}$ that

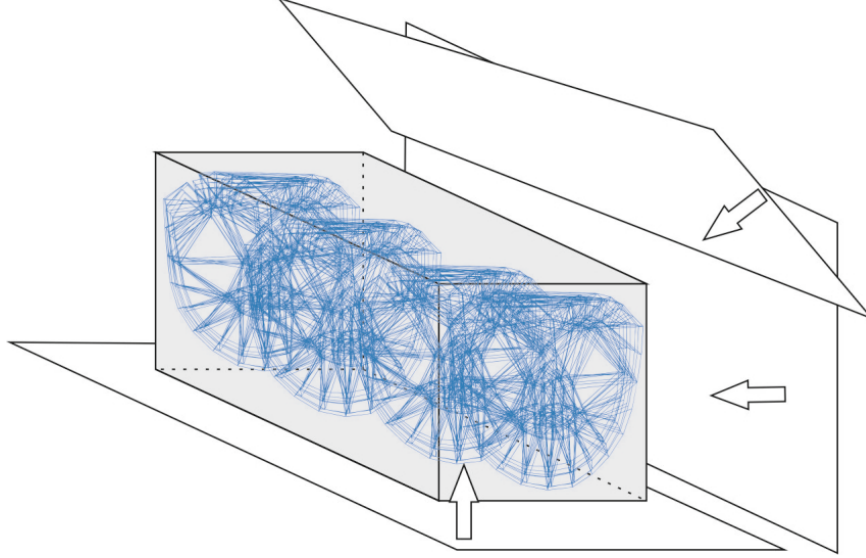


Figure 5: Illustration of three of the eight different filtrations considered.

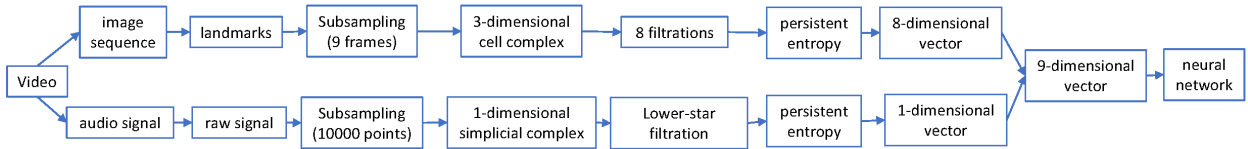


Figure 6: Summary of the workflow for emotion classification used in this paper.

assigns to each vertex of K its distance to the plane π , and to any other cell of K , the maximum distance of its vertices to the plane π . The cells are sorted according to the function values of their vertices, and then, the lower-star filtration K_π associated with the plane π is computed.

Next, the persistence diagram is computed for each of the eight filtrations. The algorithm used for this step is described in Algorithm 1 with complexity $O(n^3)$ in theory but linear in practice [Edelsbrunner and Harer, 2010, p. 159].

The persistent entropy is then computed for each of the persistence diagrams obtained. Due to its formulation, persistent entropy can be computed in linear time. As a result, an 8-dimensional vector is obtained for each image sequence.

Algorithm 1: Computing the persistence diagram for a filtration Gonzalez-Diaz and Real [2005].

Input: A filtration $\emptyset = K_0 \subset K_1 \subset K_2 \subset \dots \subset K_n = K$ and an ordering of the cells $\{\sigma_1, \dots, \sigma_m\}$ of K such that if $i < j$ then $\text{ind}(\sigma_i) < \text{ind}(\sigma_j)$ where $\text{ind}(\sigma_i) = \min\{r : \sigma_i \in K_r\}$

Output: The persistence diagram Dgm

Initialize $H = \emptyset$, $\text{Dgm} = \emptyset$, and $f(\sigma_i) = 0$ for $i \in \{1, \dots, m\}$

for $i = 1$ **to** m **do**

if $f\partial(\sigma_i) == 0$ **then**

$H \cup \{\sigma_i\}$ (a new homology class was born)

$f(\sigma_i) = \sigma_i$

$\text{Dgm} \cup \{(\text{ind}(\sigma_i), \infty)\}$

if $f\partial(\sigma_i) \neq 0$ **then**

 Let $\sigma_j \in f\partial(\sigma_i)$ such that $j == \max\{\text{ind}(\mu) : \mu \in f\partial(\sigma_i)\}$

$H \setminus \{\sigma_j\}$ (an homology class died)

foreach $x \in K$ such that $\sigma_j \in f(x)$ **do**

$f(x) = f(x) + f\partial(\sigma_i)$.

$\text{Dgm} \setminus \{(\text{ind}(\sigma_j), \infty)\} \cup \{(\text{ind}(\sigma_j), \text{ind}(\sigma_i))\}$

Finally, for each talking-face video, we add a new entry to the 8-dimensional vector computed consisting of the persistent entropy of the lower-star filtration obtained from the 1-dimensional simplicial complex computed from the raw audio signal of the video as it is done in Gonzalez-Diaz et al. [2019].

Putting all together, we obtain a 9-dimensional feature vector called the *topological signature* of the video. Moreover, thanks to the work presented in Atienza et al. [2020] we have the following result.

Lemma 1 *The so-called topological signature associated to a given talking-face video is stable in the sense that small changes in the video produce small changes in the signature.*

Proof. In Atienza et al. [2020], it is proved that persistent entropy is stable. It means that small changes in the input data produce small changes in the persistent entropy value. In this case, input data are, first, the eight filtrations obtained from the image sequence and, second the filtration obtained from the audio signal. Finally, small perturbations in the filtrations are equivalent to a small displacement of the landmark points in the image sequence or small changes in the audio signal, that is, they consists of small perturbation in the input data used to compute the persistent entropy values, concluding the proof. \square

The topological signatures computed from the talking-face video dataset are then used to train a feed-forward neural network to classify the videos into the different emotions considered.

Table 1: Comparison of our method with state-of-the-art methods.

Paper	Dataset	Average accuracy on the test set
Byun and Lee [2020]	RAVDESS	87.11%
Siddiqui and Javaid [2020]	RAVDESS	86.36%
Ma et al. [2019]	RML, enterface05, AUM-1s	77.31%
Wang et al. [2020]	RAVDESS	77.66%
Our method	RAVDESS	95.97%

4 Experimentation

For experimentation, the Ryerson Audio-Visual Database of Emotional Speech and Song (RAVDESS) is used, that is a talking-face video dataset where facial landmark points composed of 62 points have been precomputed. This dataset contains the vocalization of two statements in a neutral North American accent by 24 professional actors (12 female, 12 male). Each expression is produced at two levels of emotional intensity (normal, strong), with an additional neutral expression. The intensity fulfils an important role in emotional theory (see the works in Diener et al. [1985], Schlosberg [1954]). The strong intensity is useful when we are looking for clear emotional examples. However, as explained in Kamińska et al. [2014], the normal intensity is generally used if we are interested in providing classification for daily life. All actors produced 60 spoken expressions and 44 sung expressions. These vocalizations are available in three formats: audio-only, video-only, and audio-video. Besides, the RAVDESS video dataset contains tracked facial landmark points for all videos.

In this paper, we focus on the 60 speech videos provided in the RAVDESS video dataset. The total tracked files used is 24 actors \times 60 speeches. Since we do not consider neutral emotions to avoid an unbalanced dataset, we used a total of 1344 videos. The number of frames used as well as the number of points in the subsampled audio signal were a experimental choice consisting of the minimum number of frames and points needed to obtain good results and to develop the experiment in a feasible time. The neural network considered was the simplest one that provided satisfactory results and the weights of the neural network were tuned using a traditional training procedure.

Table 2: Confusion matrix of the audio-video experiment for one of the repetitions measured on the test dataset.

Emotion	Calm	Happy	Sad	Angry	Fearful	Disgust	Surprised
Calm	61	0	0	0	0	0	3
Happy	0	48	0	4	0	0	0
Sad	0	0	55	0	0	0	0
Angry	0	0	0	60	0	0	2
Fearful	0	0	0	0	60	0	2
Disgust	0	0	0	0	0	45	1
Surprised	0	0	0	0	4	0	55

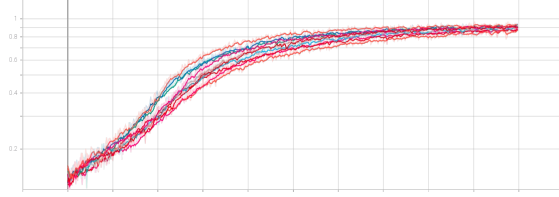


Figure 7: Accuracy values on the training set during 500 epochs. 10 repetitions.

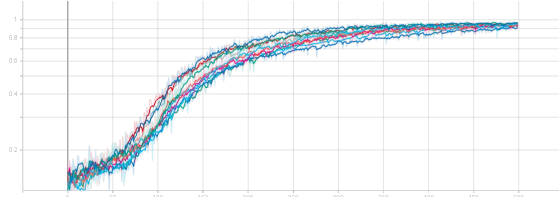


Figure 8: Accuracy values on the test dataset during 500 epochs. 10 repetitions.

The steps for the experimentation were the following (see Figure 6). We first consider the image sequence obtained for each video of the audio-video dataset. For each image sequence, 9 equally spaced frames were selected to have an appropriate representation of the full image sequence. The landmark points of those 9 frames were then used to build an 8-dimensional vector following the method described in Section 3. Then, for each video, we added a new entry to the 8-dimensional vector computed consisting of the persistent entropy of the lower-star filtration of the 1-dimensional simplicial complex obtained from a subsampling of the raw audio signal consisting of 10000 points. The subsampling process was done uniformly on the signal, maintaining its shape and main distribution of the spikes. As a result, we obtained a set of 1344 9-dimensional feature vectors, one for each video of the dataset considered.

Finally, this set was split into a training set with 944 vectors and a test set for validation with 400 vectors. Then, the training set was used to train a neural network with the following standard architecture: It is composed by 5 layers with a total of $n \times 512 \times 128 \times 64 \times 7$ neurons, using dropout (20%) in the first hidden layer with $n = 9$ being the dimension of the input (i.e., the 9-dimensional topological feature vectors). The hidden layers are composed by the ReLU activation function. Finally, the Softmax activation function is put in the output layer.

The neural network was trained during 500 epochs and the experiment was repeated 10 times using sparse categorical cross-entropy as loss function and the Adam training algorithm. The accuracy values for those repetitions are shown in Figure 7 for the training set and in Figure 8 for the test set.

The highest values reached were 99.9% of accuracy on the training set with 98.02% of accuracy on the test set. Average accuracy was 95.97% on the test set. A confusion matrix for the experiment is shown in Table 2.

The state-of-the-art methods with which we compare ours are the following ones. In Byun and Lee [2020], a model is proposed based on three deep networks that are fed using image sequences, facial landmark points and acoustic features, respectively. In Siddiqui and Javaid [2020], the fusion of visible images and infrared images with speech are used to feed an ensemble method based on convolutional neural networks. The authors in Ma et al. [2019] applied a convolutional neural network approach with a preprocessing method to eliminate data redundancy and noise. Finally, the authors in Wang et al. [2020] used convolutional and recurrent neural network together with long short-term memory. As we can see in Table 1, our method outperforms all of them.

The code developed is available at the link <https://github.com/Cimagroup/AudioVisual-EmotionRecognitionUsingTDA>. All the parameters are provided in the implementation and the replication of the experiments on the RAVDESS database can be done using the code without problem. If other dataset different to RAVDESS is used then the facial landmark points should be computed before applying the algorithm proposed in this paper.

5 Conclusions and future work

In this work, we have developed a novel method using persistent entropy and neural networks for emotion classification of talking-face videos. The results reached are promising and competitive, beating the performance reached in other state-of-the-art works found in the literature. We combined audio-signal and image-sequence information

to develop our topology-based emotion recognition method. The main drawback of our methodology is the need of a video long enough to be able to select a representative subset of frames to compute the cell complex. This fact makes our method not useful in real-time applications.

The following future works are plan to be explored: To expand the topological signature by extracting more information from the audio signals. To divide the landmark points into different subsets to determine regions or pairs of regions that contain discriminative landmark points for each facial expression. To use the the 3-dimensional information provided by the landmark points. To take advantage of the depth information of the landmark points could be a challenging problem for the future together with considering higher dimensional topological information once that we increase the dimension of the data we are dealing with.

References

- Nieves Atienza, Rocio Gonzalez-Diaz, and Manuel Soriano-Trigueros. On the stability of persistent entropy and new summary functions for topological data analysis. *Pattern Recognition*, 107:107509, 2020. ISSN 0031-3203.
- Egils Avots, Tomasz Sapiński, Maie Bachmann, and Dorota Kamińska. Audiovisual emotion recognition in wild. *Machine Vision and Applications*, 30(5):975–985, 2019.
- Jacopo Binchi, Emanuela Merelli, Matteo Rucco, Giovanni Petri, and Francesco Vaccarino. jholes: A tool for understanding biological complex networks via clique weight rank persistent homology. *Electron. Notes Theor. Comput. Sci.*, 306:5–18, 2014.
- Sung-Woo Byun and Seok-Pil Lee. Human emotion recognition based on the weighted integration method using image sequences and acoustic features. *Multimedia Tools and Applications*, pages 1–15, 09 2020.
- Frédéric Chazal, Brittany Terese Fasy, Fabrizio Lecci, Alessandro Rinaldo, Aarti Singh, and Larry Wasserman. On the bootstrap for persistence diagrams and landscapes. *odel. Anal. Inform. Syst.*, 20(6):111–120, 2013.
- Harish Chintakunta, Thanos Gentimis, Rocio Gonzalez-Diaz, Maria-Jose Jimenez, and Hamid Krim. An entropy-based persistence barcode. *Pattern Recognition*, 48(2):391 – 401, 2015. ISSN 0031-3203.
- Yu-Min Chung, Chuan-Shen Hu, Yu-Lun Lo, and Hau-Tieng Wu. A persistent homology approach to heart rate variability analysis with an application to sleep-wake classification. *Frontiers in Physiology*, 12:202, 2021. ISSN 1664-042X.
- Ed Diener, Randy J Larsen, Steven Levine, and Robert A Emmons. Intensity and frequency: dimensions underlying positive and negative affect. *Journal of personality and social psychology*, 48(5):1253, 1985.
- Herbert Edelsbrunner and John Harer. *Computational topology: an introduction*. American Mathematical Soc., 2010.
- Rocio Gonzalez-Diaz and Pedro Real. On the cohomology of 3d digital images. *Discrete Applied Mathematics*, 147(2-3):245–263, 2005.
- Rocio Gonzalez-Diaz, Eduardo Paluzo-Hidalgo, and José F. Quesada. Towards emotion recognition: A persistent entropy application. In *Int. Conf. on Computational Topology in Image Context*, pages 96–109, 2019.
- Xin Guo, Luisa F Polanía, and Kenneth E Barner. Audio-video emotion recognition in the wild using deep hybrid networks. *arXiv preprint arXiv:2002.09023*, 2020.
- Simon S. Haykin. *Neural networks and learning machines*. Pearson Education, Upper Saddle River, NJ, third edition, 2009.
- Dias Issa, M Fatih Demirci, and Adnan Yazici. Speech emotion recognition with deep convolutional neural networks. *Biomedical Signal Processing and Control*, 59:101894, 2020.
- Robert Jenke, Angelika Peer, and Martin Buss. Feature extraction and selection for emotion recognition from eeg. *IEEE Trans. on Affective computing*, 5(3):327–339, 2014.
- Dorota Kamińska, Tomasz Sapiński, and Adam Pelikant. Recognition of emotion intensity basing on neutral speech model. In *Man-Machine Interactions 3*, pages 451–458. Springer, 2014.
- Diederik P. Kingma and Jimmy Ba. Adam: A method for stochastic optimization, 2017.
- Andrea Kleinsmith and Nadia Bianchi-Berthouze. Affective body expression perception and recognition: A survey. *IEEE Trans. on Affective Computing*, 4(1):15–33, 2012.
- Jean Kossaifi, Georgios Tzimiropoulos, Sinisa Todorovic, and Maja Pantic. A few-va database for valence and arousal estimation in-the-wild. *Image and Vision Computing*, 65:23–36, 2017.
- Boris Kryzhanovsky, Witali Dunin-Barkowski, and Vladimir Redko. Advances in neural computation, machine learning, and cognitive research. *Neuroinformatics*, 2017.

- Soonil Kwon et al. Mlt-dnet: Speech emotion recognition using 1d dilated cnn based on multi-learning trick approach. *Expert Systems with Applications*, 167:114177, 2021.
- J. Lamar-Leon, R. Alonso-Baryolo, E. Garcia-Reyes, and R. Gonzalez-Diaz. Persistent homology-based gait recognition robust to upper body variations. In *2016 23rd Int. Conf. on Pattern Recognition*, pages 1083–1088, 2016.
- Javier Lamar-León, Andrea Cerri, Edel B. García Reyes, and Rocio Gonzalez-Diaz. Gait-based gender classification using persistent homology. In *Progress in Pattern Recognition, Image Analysis, Computer Vision, and Applications - 18th Iberoamerican Congress, CIARP 2013, Havana, Cuba*, volume 8259 of *LNCS*, pages 366–373. Springer, 2013.
- Javier Lamar-León, Raul Alonso Baryolo, Edel B. García Reyes, and Rocio Gonzalez-Diaz. Topological features for monitoring human activities at distance. In *Activity Monitoring by Multiple Distributed Sensing - 2nd Int. Workshop, AMMDS 2014, Stockholm, Sweden*, volume 8703 of *LNCS*, pages 40–51. Springer, 2014.
- Steven R. Livingstone and Frank A. Russo. The ryerson audio-visual database of emotional speech and song (ravdess): A dynamic, multimodal set of facial and vocal expressions in north american english. *PLOS ONE*, 13(5):1–35, 05 2018.
- Yaxiong Ma, Yixue Hao, Min Chen, Jincan Chen, Ping Lu, and Andrej Košir. Audio-visual emotion fusion (avef): A deep efficient weighted approach. *Information Fusion*, 46:184–192, 2019. ISSN 1566-2535.
- Emanuela Merelli, Marco Piangerelli, Matteo Rucco, and Daniele Toller. A topological approach for multivariate time series characterization: the epileptic brain. In *Procs. of the 9th EAI Int. Conf. on Bio-inspired Information and Communications Technologies (formerly BIONETICS)*, pages 201–204, 2016.
- Elizabeth Munch, Katharine Turner, Paul Bendich, Sayan Mukherjee, Jonathan Mattingly, John Harer, et al. Probabilistic fréchet means for time varying persistence diagrams. *Electronic Journal of Statistics*, 9(1):1173–1204, 2015.
- Audun Myers, Elizabeth Munch, and Firas A. Khasawneh. Persistent homology of complex networks for dynamic state detection. *Phys. Rev. E*, 100:022314, Aug 2019.
- Fatemeh Noroozi, Dorota Kaminska, Ciprian Corneanu, Tomasz Sapinski, Sergio Escalera, and Gholamreza Anbarjafari. Survey on emotional body gesture recognition. *IEEE Trans. on affective computing*, 2018.
- Ikechukwu Ofofiele, Kaustubh Kulkarni, Ciprian Adrian Corneanu, Sergio Escalera, Xavier Baro, Sylwia Hyniewska, Juri Allik, and Gholamreza Anbarjafari. Automatic recognition of deceptive facial expressions of emotion. *arXiv preprint arXiv:1707.04061*, 2, 2017.
- Paweł Pławiak, Tomasz Sońnicki, Michał Niedźwiecki, Zbysław Tabor, and Krzysztof Rzecki. Hand body language gesture recognition based on signals from specialized glove and machine learning algorithms. *IEEE Trans. on Industrial Informatics*, 12(3):1104–1113, 2016.
- Matteo Rucco, Rocio Gonzalez-Diaz, Maria-Jose Jimenez, Nieves Atienza, Cristina Cristalli, Enrico Concettoni, Andrea Ferrante, and Emanuela Merelli. A new topological entropy-based approach for measuring similarities among piecewise linear functions. *Signal Processing*, 134:130–138, 2017.
- Matteo Rucco, Giovanna Viticchi, and Lorenzo Falsetti. Towards personalized diagnosis of glioblastoma in fluid-attenuated inversion recovery (flair) by topological interpretable machine learning. *Mathematics*, 8(5), 2020.
- Tomasz Sapiński, Dorota Kamińska, Adam Pelikant, Cagri Ozcinar, Egils Avots, and Gholamreza Anbarjafari. Multimodal database of emotional speech, video and gestures. In *Int. Conf. on Pattern Recognition*, pages 153–163. Springer, 2018.
- Harold Schlosberg. Three dimensions of emotion. *Psychological review*, 61(2):81, 1954.
- Seyedehsamaneh Shojaeilangari, Wei-Yun Yau, and Eam-Khwang Teoh. Pose-invariant descriptor for facial emotion recognition. *Machine Vision and Applications*, 27(7):1063–1070, 2016.
- Mohammad Faridul Haque Siddiqui and Ahmad Y. Javaid. A multimodal facial emotion recognition framework through the fusion of speech with visible and infrared images. *Multimodal Technologies and Interaction*, 4(3), 2020.
- Nitish Srivastava, Geoffrey Hinton, Alex Krizhevsky, Ilya Sutskever, and Ruslan Salakhutdinov. Dropout: A simple way to prevent neural networks from overfitting. *J. Mach. Learn. Res.*, 15(1):1929–1958, January 2014. ISSN 1532-4435.
- Csaba D Toth, Joseph O’Rourke, and Jacob E Goodman. *Handbook of discrete and computational geometry*. CRC press, 2017.
- Katharine Turner, Yuriy Mileyko, Sayan Mukherjee, and John Harer. Fréchet means for distributions of persistence diagrams. *Discrete & Computational Geometry*, 52(1):44–70, 2014.

- Jun Wan, Sergio Escalera, Gholamreza Anbarjafari, Hugo Jair Escalante, Xavier Baró, Isabelle Guyon, Meysam Madadi, Juri Allik, Jelena Gorbova, Chi Lin, et al. Results and analysis of chlearn lap multi-modal isolated and continuous gesture recognition, and real versus fake expressed emotions challenges. In *Procs. of the IEEE Int. Conf. on Computer Vision Workshops*, pages 3189–3197, 2017.
- Xupeng Wang, Ferdous Sohel, Mohammed Bennamoun, Yulan Guo, and Hang Lei. Scale space clustering evolution for salient region detection on 3d deformable shapes. *Pattern Recognition*, 71:414–427, 2017.
- Xusheng Wang, Xing Chen, and Congjun Cao. Human emotion recognition by optimally fusing facial expression and speech feature. *Signal Processing: Image Communication*, 84:115831, 2020. ISSN 0923-5965.
- Biqiao Zhang, Georg Essl, and Emily Mower Provost. Recognizing emotion from singing and speaking using shared models. In *2015 Int. Conf. on affective computing and intelligent interaction (acii)*, pages 139–145. IEEE, 2015.
- A. Zomorodian and G. Carlsson. Computing persistent homology. *Discrete and Computational Geometry*, 33(2): 249–274, 2005.